Twenty-First Symposium (International) on Combustion/The Combustion Institute, 1986 pp. 1719–1727

ABSOLUTE CONCENTRATION MEASUREMENTS OF OH IN LOW-PRESSURE HYDROGEN-OXYGEN, METHANE-OXYGEN, AND ACETYLENE-OXYGEN FLAMES

K. KOHSE-HÖINGHAUS, P. KOCZAR, TH. JUST
Institut für Physikalische Chemie der Verbrennung,
DFVLR,
Pfaffenwaldring 38, 7000 Stuttgart 80,
West Germany

Corresponding OH concentration and temperature profiles were determined for a variety of low-pressure flames using the method of laser-induced saturated fluorescence as described earlier by the authors.
For the example of a well-characterized $H_2 - O_2 - Ar$ flame, the parameters influencing the accuracy of species concentration and temperature measurements are discussed in detail. Good agreement with both literature data and a chemical-kinetic computer model was obtained. The temperature was shown to be a sensitive parameter in the modelling.
For different flame conditions, OH concentration and temperature profiles in $CH_4 - O_2$ and $C_2H_2 - O_2$ flames are reported which may be used for detailed comparisons with chemical-kinetic flame models.

Introduction

Experimental data on species concentration and temperature distribution in low-pressure flames may contribute to the understanding of the chemistry of combustion processes. To test kinetic flame models, reliable absolute concentration profiles of important intermediates are needed. Laser-induced fluorescence (LIF) is well suited for the determination of radical concentrations[1–5]. Recently, we tested and refined the method of saturated LIF[6,7] considering possible sources of uncertainties. We performed experiments and calculations concerning the validity of a two-level formalism, the influence of inhomogeneous saturation in the observation volume, and the calibration of the optical detection system. As radical source for these investigations, we used a small burner which had not been especially designed for kinetic purposes. Since low pressure and a small burner diameter may have caused a non-negligible amount of radial diffusion, a larger burner was constructed for further study and application of the saturated LIF method. In the present report, temperature and OH concentration profiles are described for different fuels under flame conditions suitable for the comparison with a one-dimensional flame model.

Experimental

The apparatus used for this investigation was a standard type for time-resolved fluorescence measurements. Single line excitation by a nanosecond pulse of a frequency-doubled dye laser (Quanta Ray), and single line detection with a 0.6 m monochromator (Jobin Yvon), photomultiplier, and fast transient digitizer (Tektronix *R* 7912) were employed. Important experimental conditions were controlled by a minicomputer (PDP 11/34), which also served for data acquisition and evaluation. Details of the experimental arrangement have been given in Ref. 6,7. We used a burner with a brass plate of 42 mm diameter which had approximately 750 1 mm diameter holes. The burner could be moved vertically and laterally. Figure 1 shows typical radial OH profiles obtained with this burner for different heights h above the burner surface. The flame conditions for the different fuels are listed in Table I.

Results and Discussion

1. Hydrogen-Oxygen Flames

It is well known that the OH concentration in flat hydrogen-oxygen flames can be reliably

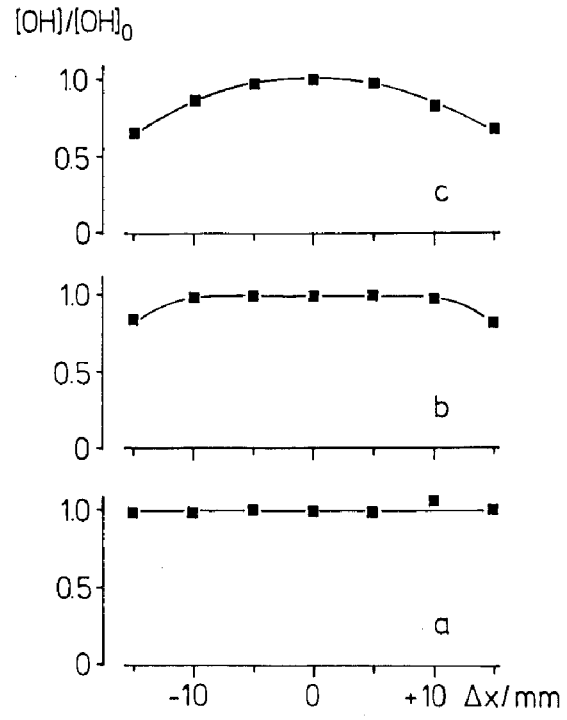

FIG. 1. Radial OH concentration profiles for a burner translation of $x = \pm 15$ mm from the center at different heights h above the burner surface a: $h = 4$ mm; b: $h = 10$ mm; c: $h = 20$ mm

simulated by one-dimensional flame kinetic models. A detailed comparison for several low-pressure $H_2 - O_2$ flames diluted with argon has been given by Lucht and Laurendeau[3]. We have chosen one of their flame conditions adapted to our burner diameter (see Table I, flame I) for a thorough analysis of our experimental procedure, as well as for a test of the computer code[8] and kinetic data we employed for the simulation.

Our approach of evaluating absolute radical number densities from saturated fluorescence data has been described in detail in Ref. 7. Here, only some major points influencing the accuracy of the concentration measurements are given.

The radical number density N_T is expressed as follows:

$$N_T = \frac{1}{f_T} \cdot \frac{I \cdot 4\pi}{V \cdot \Omega_0 \cdot A_{21} \cdot h \cdot \nu_{21}} \qquad (1)$$

where f_T is the Boltzmann factor corresponding to the measured local flame temperature T in the observation volume. I is the fluorescence intensity in the solid angle Ω_o determined in absolute units by a calibration of the efficiency of the optical detection system. A_{21} is the Einstein coefficient for the fluorescence radiation of frequency ν_{21}. V is a spatial integral and includes the influence of inhomogenous saturation in the observation volume (see Ref. 7). To obtain V, the population differential equation must be solved separately for each volume element, taking into consideration the different intensities of the center and wings of the spatial laser beam profile. Next, an integration over the beam cross section has to be performed. V has the dimension of a volume. Furthermore, V is a function of the fluorescence decay rate α, which may be evaluated from the time-resolved fluorescence signal.

In summary, the accuracy of the radical concentration measurement is mainly determined by correct consideration of the spatial laser beam profile ("wing") effects and by the accuracy of the calibration of the optical detection efficiency. Additionally, the influence of quenching and relaxation, which may be dependent on the local chemical environment in

TABLE I
Flame Conditions

Flame		p [mbar]	ϕ	flow rates [cm^3 NTP/min]					
I	$H_2 - O_2 - Ar$	95	0.6	H_2	485	O_2	405	Ar	1520
II	$H_2 - O_2$	40	1.2		2535		1055		
III	$CH_4 - O_2$	40	0.6	CH_4	830	O_2	2760		
IV			1.2		1345		2245		
V			1.6		1595		1995		
VI			1.2		562		938		
VII	$C_2H_2 - O_2$	40	0.6	C_2H_2	695	O_2	2895		
VIII			1.2		1165		2425		
IX			1.6		1400		2190		

the flame, has to be examined. The next figures will illustrate these relations by some typical results which were obtained in the hydrogen-oxygen flames. The course of the experimental investigation for the hydrocarbon flames is similar and will be described later.

Figure 2 illustrates the inhomogeneous saturation effects. The integral V has been evaluated as a function of the laser intensity expression $u = u_{\nu,\max} \cdot B_{21}$ (Ref. 7) by taking its measured spatial, temporal and spectral distribution into account. From this calculated V curve which matches the experimental conditions, the average saturation degree S has been calculated and compared with measured values (for details, see Ref. 7). S describes the average saturation in the observation volume, which may be probed by inserting a filter into the laser beam. Here, a filter with 30 % transmission was used. The circles are measured average saturation degrees given by the ratios of the fluorescence intensities with and without the filter in the laser beam for different laser intensities u.

For each measured saturation degree S, a corresponding value of V is determined. For the same experimental points, the ratio of the fluorescence intensity I and the integral V is plotted in the lower part of Fig. 2. The expression I/V is proportional to the radical number density (see Eq. 1). The scatter of I/V reflects the overall accuracy of the evaluated concentrations. The error bars in Fig. 2 indicate a statistical error of ± 20 %, which includes errors in the determination of the laser intensity, the fluorescence intensity, the observation volume, and the fluorescence decay rate, and which is typical for the low-pressure flames investigated.

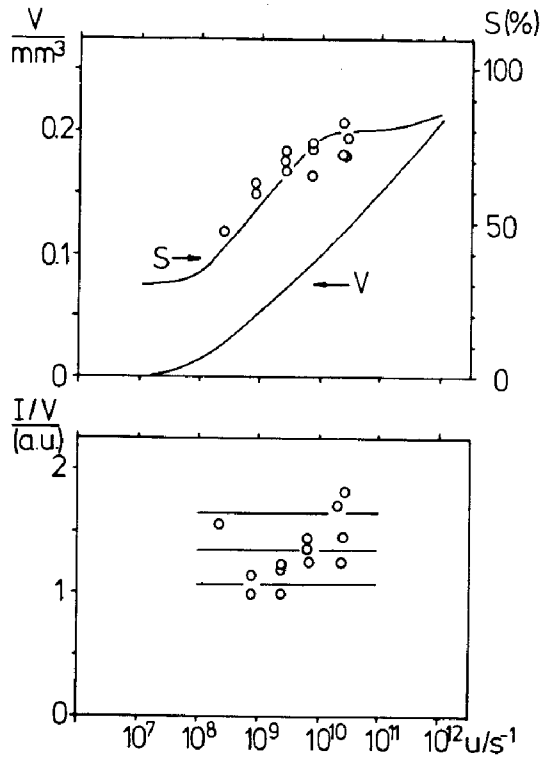

FIG. 2. Top: Integral V and saturation degree S vs. laser intensity u; ○ measured average saturation degrees at h = 10 mm above the burner surface in a 95 mbar, ϕ = 0.6 H_2 − O_2 − Ar flame (flame I) Bottom: Ratio of fluorescence intensity I and integral V vs. laser intensity u for the same measured values as above. The error bars indicate one standard deviation of ± 20 %.

As already discussed, the calibration of the optical detection efficiency is important for accurate absolute concentration measurements by LIF. We employ two independent ways for the calibration. The first method uses a calibration pulse which is produced by scattering the laser beam at the surface of a grounded quartz disk, mounted on the burner head. The intensity of this calibration pulse can be measured (see Ref. 7), and thus we determine the overall efficiency factor for the optical detection system. The second method uses the Raman scattered light of the Q branch of nitrogen for the calibration; the cross section for this Raman process is well-known[9].

The agreement for these two methods is shown in Fig. 3, where the calibration factors

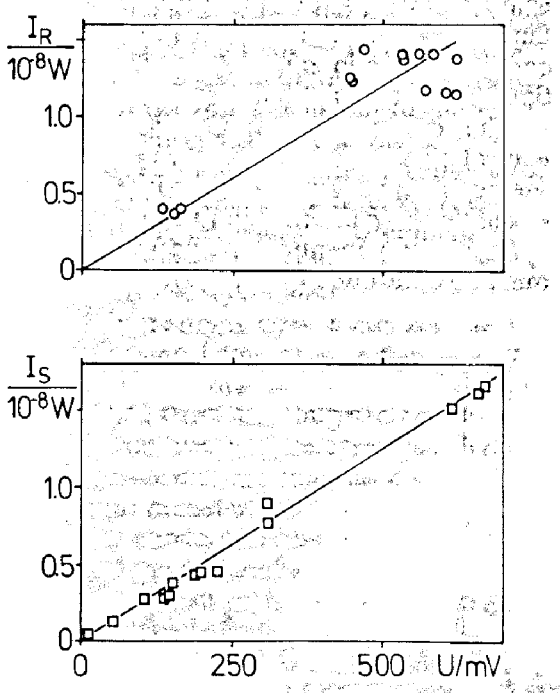

FIG. 3. Calibration of the optical detection system. Top: Raman method; the linear regression results in a calibration factor of (2.4 ± 0.2) · 10^{-11} W/mV. Bottom: Quartz disk method, the linear regression giving a calibration factor of (2.5 ± 0.1) · 10^{-11} W/mV.

are displayed for the range of laser intensities used in the fluorescence experiment. It is essential to perform the calibration for the same spectral and geometrical conditions as for the fluorescence measurements. The Raman results are shown in the upper part of Fig. 3. A calibration factor of $(2.4 \pm 0.2) \cdot 10^{-11}$ W/mV is obtained which allows us to transform the recorded fluorescence signal in mV to an absolute scale. With the quartz disk method, a calibration factor of $(2.5 \pm 0.1) \cdot 10^{-11}$ W/mV is determined, as shown in the lower part of Fig. 3. This quite satisfactory agreement of the calibration factors given by the two procedures is only achieved with a very careful alignment of the optical detection system.

If the influence of collision processes varies strongly with the position in the flame or with the equivalence ratio, local fluorescence decay rates must be taken into account in determining radical number densities. For the low-pressure flames, the decay rate α can be measured directly from the time-resolved fluorescence signals. Figure 4 shows the variation of α with height above the burner surface for a 40 mbar, $\phi = 1.2$ $H_2 - O_2$ flame (flame II): α increases slightly in the direction of the burnt gases. This variation is so small, however, that it need not be considered for the nearly saturated fluorescence conditions of the experiment. The mean value of $1.5 \cdot 10^8$ s^{-1} was used in this case. Similarly, we measured the influence of the equivalence ratio on the decay rate. For all flames listed in Table I, the combined variation of the corresponding α with position and equivalence ratio was less than $\pm$ 30 %, so that the average of α could always be used for the evaluation of concentration profiles.

As already mentioned, local temperatures must be determined with the highest precision

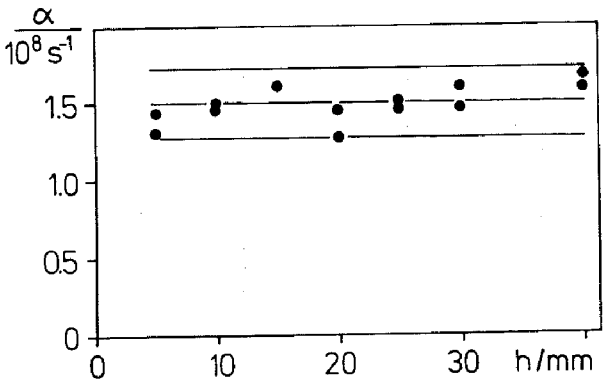

FIG. 4. Decay constant α vs. height above the burner surface h for a 40 mbar, $\phi = 1.2$ $H_2 - O_2$ flame (flame II), indicating a deviation of $\pm$15 % from the average value of $1.5 \cdot 10^8$ s^{-1}.

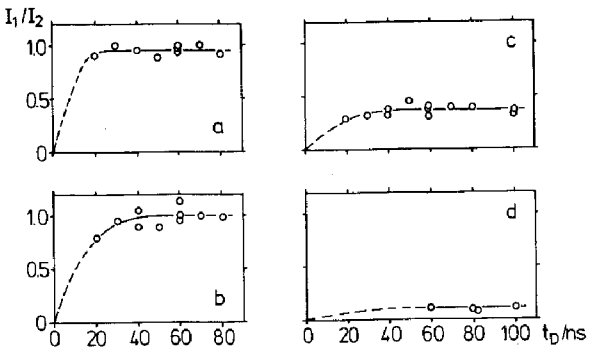

FIG. 5. Thermalization of OH: intensity ratios I_1/I_2 of different line pairs vs. delay time t_D (flame I). *a-c:* Q_1 (6) excitation, *d:* P_1 (9) excitation
a: I (Q_1 (4))/I (Q_1 (5))
b: I (P_1 (11))/I (Q_1 (4))
c: I (P_2 (10))/I (P_1 (11))
d: I (Q_1 (15))/I (Q_1 (5))

possible. Our LIF temperatures are measured in the following way. A particular transition of the OH ($A^2\Sigma^+ - X^2\Pi$, 0–0) band is excited. Then, we wait for a certain time, until the population has thermalized. The appropriate delay time is obtained by monitoring intensity ratios of different line pairs until they remain constant. An example for this is given in Fig. 5 for a 95 mbar $\phi = 0.6$ $H_2 - O_2 - Ar$ flame (flame I). In the diagrams *a–c*, thermalization upon excitation of Q_1 (6) is measured, for diagram *d*, P_1 (9) excitation was used. From these curves and some additional line pairs not shown here, a delay time of at least 60 ns was chosen for this flame. This delay time corresponds to the particular collisional conditions in flame I; for lower pressures (13 mbar), delay times of more than 200 ns may be obtained. The temperature was then determined from rotational spectra measured after a suitable delay time. Temperatures from spectra using different excitation lines always agreed within experimental error.

The temperatures and OH number densities obtained for the 95 mbar $\phi = 0.6$ $H_2 - O_2 - Ar$ flame (flame I) are shown in Fig. 6. The temperatures were measured following Q_1 (6) and P_1 (9) excitation; the typical error limits are $\pm$ 55 K. For a comparison with the flame model, two different temperature profiles were chosen, which both represent the measured values within experimental error. They are indicated by the solid and broken line. In the lower part of Fig. 6, the OH mole fractions corresponding to these two temperature profiles are shown as large filled and small open circles. They do not coincide, as the Boltzmann fraction and the total number density in the

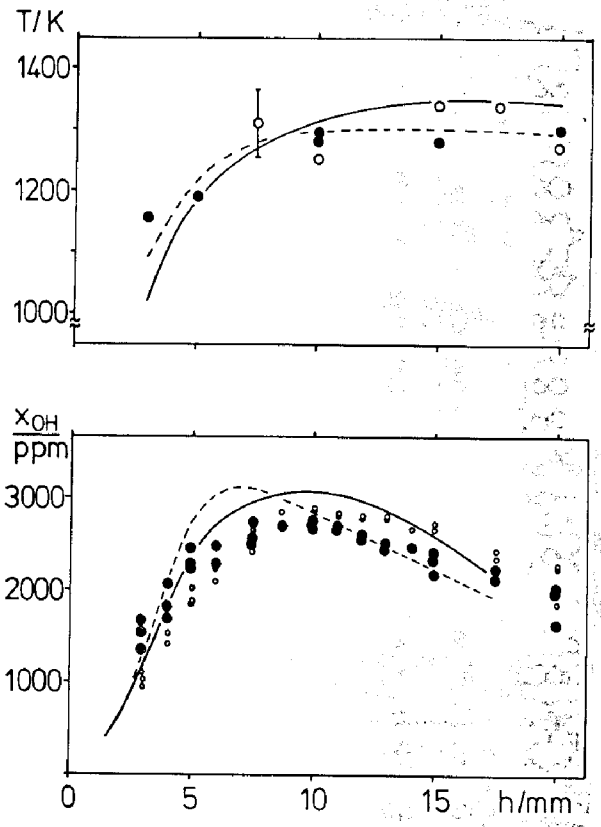

FIG. 6. Temperature (top) and OH concentration (bottom) vs. height above the burner surface h in a 95 mbar, $\phi = 0.6\ H_2 - O_2 - Ar$ flame (flame *I*). *Top:* • Q_1 (6) excitation, ○ P_1 (9) excitation, error bars ± 55 K. The indicated temperature profiles have been used as input for the flame model. *Bottom:* Measured (•) and simulated (—) OH mole fraction corresponding to the solid temperature curve; measured (○) and simulated (---) OH mole fraction corresponding to the broken temperature curve.

flame change with temperature. Therefore, the same measured fluorescence intensities result in different mole fractions for different temperatures.

Both slightly different temperature profiles were used as input for the flame model[8], in order to simulate the experimental OH concentration profile. The kinetic model parameters are mainly those recommended by Warnatz[10]. For the very important reaction of the H atom with O_2, the rate constant of Frank and Just[11] was used. Furthermore, the rate constants for some HO_2 reactions were chosen differently. We have taken the values given by Braun et al.[12], Sridharan et al.[13], and Baulch et al.[14] for the reactions of HO_2 with OH, O, and H, respectively. With the entire set of kinetic parameters described here, the computer model was tested for some hydrogen – oxygen flames reported in the literature[3,15–17]. For the very different flame conditions ranging from the 7 mbar flame of Homann[15] to the atmospheric pressure flame of Goldsmith[17], simulated OH concentrations were found in good agreement with the experiment. For the three different flame conditions of Lucht and Laurendeau[3], the OH concentrations and also the relative H atom profiles given in Ref.[18] were well reproduced by the flame model.

The simulated OH concentrations obtained for our experiment with the two slightly different temperature profiles are shown in Fig. 6. The broken line corresponds to the broken temperature profile and should be compared with the experimental OH mole fraction given by the small open circles; the solid line corresponds to the solid temperature curve and should be compared with the filled circles. It can be seen that the maximum OH concentrations given by the calculations are practically the same, but they occur at different positions. Both sets of experimental and calculated OH concentrations agree within experimental error, but the solid line gives a somewhat better representation of the measured OH data. It should be stressed, however, that the choice of the two temperature profiles is arbitrary within the experimental accuracy. This example simply demonstrates the great influence of a small change in temperature on the simulated OH concentrations. A systematic sensitivity analysis for this flame has revealed that practically only the reaction $H + O_2 + M \rightarrow HO_2 + M$ has a definite influence on the simulated OH profile. This reaction is strongly coupled to the set of radical producing reactions such as $H + O_2 \rightleftarrows OH + O$ etc. We conclude that the local temperature must be measured very carefully if a reliable kinetic modelling is attempted even for a system which has a simple chemistry like the hydrogen – oxygen flame.

Similar observations were made for the hydrogen – oxygen flame at 40 mbar, $\phi = 1.2$ (flame II). Here, a higher maximum temperature was found, corresponding to an increase in OH concentration. The results for both hydrogen – oxygen flames are summarized in Table II. The kinetic model with the set of parameters as described above was also suitable for the simulation of the OH profile measured in flame II; good agreement with the experiment was obtained.

2. *Methane – Oxygen Flames*

A variety of methane flame investigations is found in the literature, (see for example Ref. 19–25). Mostly, OH concentration or temperature measurements were performed in atmos-

TABLE II
Maximum OH concentrations and temperatures in hydrogen – oxygen flames

Flame	ϕ	T [K]	N_{OH} [cm^{-3}]	x_{OH}[ppm]
I	0.6	1350	$1.4 \cdot 10^{15}$	2700
II	1.2	1500	$2.0 \cdot 10^{15}$	10300

pheric pressure methane – air flames[21,22,24,25]. Only a limited range of flame conditions have been used for most of the experiments. For equivalence ratios close to stoichiometric in an atmospheric CH_4 –air flame, Cattolica found good agreement of measured OH concentrations with a kinetic flame model[24].

Here, we report OH concentration and temperature profiles in several low-pressure CH_4 – O_2 flames for the conditions shown in Table I. Concentrations and temperatures were measured following the same procedure as for the hydrogen – oxygen flames and the same care was taken to ensure the reliability of these measurements. Table III summarizes the results. The OH mole fraction and the temperature, as functions of height above the burner surface, are shown in Fig. 7 for two slightly rich CH_4 – O_2 flames with different unburnt gas velocities (flames IV and VI). As expected, the flame temperature decreases with decreasing flow velocity, resulting in a much lower OH concentration. Fig. 8 shows the OH concentration and temperature profiles for a lean and a rich CH_4 – O_2 flame (flames III and V). Comparison with a kinetic flame model is desirable and will be pursued.

3. *Acetylene – Oxygen Flames*

Concentration measurements for OH in low pressure acetylene – oxygen flames have been reported by Eberius et al.[26] and Vandooren and Van Tiggelen[27] for a limited range of flame conditions. We performed OH concentration and temperature measurements as already described. Three C_2H_2 – O_2 flames with different equivalence ratios were investigated. The flame conditions are listed in Table I; Fig. 9 and Table IV show the results. In this case, temperatures determined from OH rotational spectra were checked by measuring CH temperatures for the slightly rich flames at the position of the maximum CH fluorescence intensity; they were in good agreement with the OH temperatures. This experiment additionally delivered an estimate of the CH concentrations in the three acetylene – oxygen flames. As an example, the CH concentration profile for flame VIII is included in Fig. 9, the CH maximum at 1.9 mm is 27.5 ppm. The CH concentration profiles are in good qualitative agreement with those recently reported by Joklik et al.[28].

For the OH concentrations shown in Table IV and Fig. 9, the maximum occurs under near stoichiometric conditions. In the lean flame, the OH concentration is slightly lower. For the rich flame, a considerable decrease in OH concen-

TABLE III
Maximum OH concentrations and temperatures in methane – oxygen flames

Flame	ϕ	T [K]	N_{OH} [cm^{-3}]	x_{OH} [ppm]
III	0.6	2100	$3.2 \cdot 10^{15}$	22500
IV	1.2	1900	$3.2 \cdot 10^{15}$	21000
V	1.6	1950	$1.1 \cdot 10^{15}$	7300
VI	1.2	1575	$2.0 \cdot 10^{15}$	10500

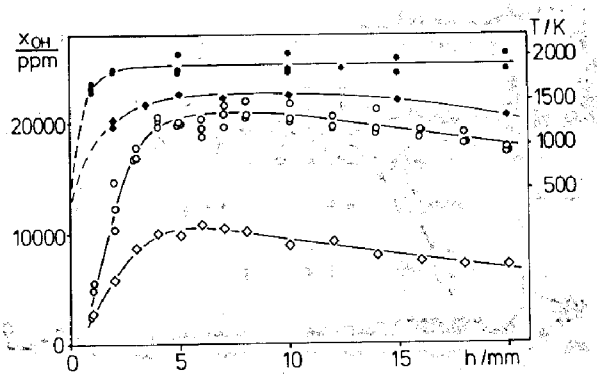

FIG. 7. Temperature T and OH mole fraction x_{OH} vs. height above the burner surface h for two 40 mbar, $\phi = 1.2$ CH_4 – O_2 flames; ○ x_{OH}, ● T, flame IV; ◇ x_{OH}, ◆ T, flame VI.

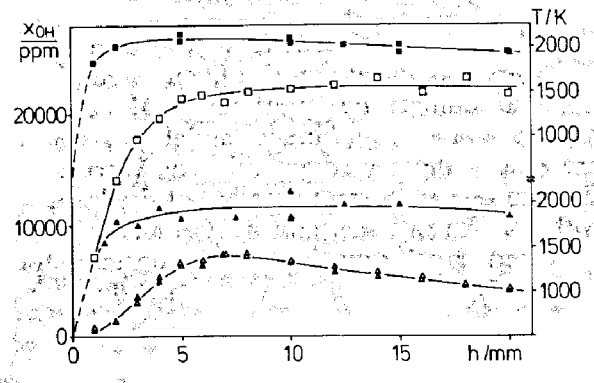

FIG. 8. Temperature T and OH mole fraction x_{OH} vs. height above the burner surface h for two 40 mbar CH_4 – O_2 flames; □ x_{OH}, ■ T, $\phi = 0.6$, flame III; △ x_{OH}, ▲ T, $\phi = 1.6$, flame V.

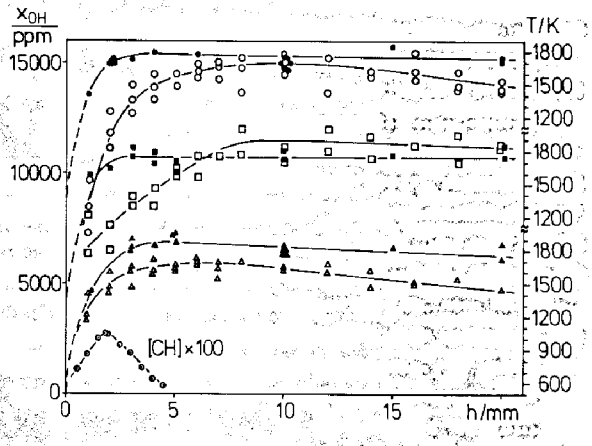

FIG. 9. Temperature T and OH mole fraction x_{OH} vs. height above the burner surface h for three 40 mbar $C_2H_2 - O_2$ flames; ○ x_{OH}, ● T, $\phi = 1.2$, flame VIII; □ x_{OH}, ■ T, $\phi = 0.6$, flame VII; △ x_{OH}, ▲ T, $\phi = 1.6$, flame IX. Additionally, the CH mole fraction measured in flame VIII is displayed (⊙); the CH maximum is 27.5 ppm.

tration is observed. A similar course of OH concentration with equivalence ratio had been noticed in earlier investigations[6,7] for the 13 mbar C_2H_2–O_2 flames stabilized on a smaller burner. Although the chemistry of the acetylene – oxygen system is highly complex and seems to suffer from incomplete knowledge of important kinetic steps, an attempt is planned to simulate the reported OH concentrations using the kinetic flame model.

Conclusions

OH concentration and temperature profiles have been measured by saturated laser-induced fluorescence for three different fuels and a range of equivalence ratios. The conditions were chosen to be suitable for the comparison with a one-dimensional chemical-kinetic flame model.

The measurement procedure has been discussed and the parameters which determine the experimental accuracy were demonstrated in a detailed analysis of the hydrogen-oxygen flame. Regarding the simple kinetics of this flame, a computer simulation with a one-dimensional model was carried out. Experiments and simulations agreed satisfactorily. Using slightly different experimental temperature profiles as input parameters for the flame model, a relatively strong influence on the modeled OH concentration profile was observed. Great care is needed in determining the local temperatures when experiments are used to check finer details of flame models for laminar flames.

Two hydrocarbon flames were investigated for different conditions. In particular for acetylene flames, a complete picture describing the combustion chemistry is not yet available from the literature. The OH concentration and temperature profiles reported here are similar concerning accuracy and reproducibility as demonstrated for the hydrogen – oxygen system. They may serve as one base for improved kinetic modelling.

TABLE IV
Maximum OH concentrations and temperatures in acetylene-oxygen flames

Flame	ϕ	T [K]	N_{OH} [cm^{-3}]	X_{OH} [ppm]
VII	0.6	1750	$1.9 \cdot 10^{15}$	11200
VIII	1.2	1780	$2.4 \cdot 10^{15}$	15000
IX	1.6	1890	$9.3 \cdot 10^{14}$	6000

Acknowledgements

We thank Dr. S. Kelm for performing the calculations with the chemical-kinetic flame model. Technical help of Mr. Ch. Wolter with some of the experiments is gratefully acknowledged.

REFERENCES

1. DAILY, J.W.: Appl. Opt. *16*, 568 (1977)
2. SMITH, G.P. AND CROSLEY, D.R.: Eighteenth Symposium (International) on Combustion, p. 1511, The Combustion Institute, 1981
3. LUCHT, R.P., SWEENEY, D.W. AND LAURENDEAU, N.M.: Comb. Flame *50*, 189 (1983)
4. STEPOWSKI, D. AND COTTEREAU, M.J.: Appl. Opt. *18*, 354 (1979)
5. ECKBRETH, A.C.: Eighteenth Symposium (International) on Combustion, p. 1471, The Combustion Institute, 1981
6. KOHSE-HÖINGHAUS, K., PERC, W. AND JUST, Th.: Ber. Bunsenges. Phys. Chem. *87*, 1052 (1983)
7. KOHSE-HÖINGHAUS, K., HEIDENREICH, R. AND JUST, Th.: Twentieth Symposium (International) on Combustion, p. 1177, The Combustion Institute, 1984
8. J. WARNATZ kindly provided us with a copy of his one-dimensional flame program.
9. SCHRÖTTER, H.W. AND KLÖCKNER, H.W.: Raman Spectroscopy of Gases and Liquids (A. Weber, Ed.), Topics in Current Physics Vol. 11, p. 123, Springer, Berlin, 1979
10. WARNATZ, J.: Combustion Chemistry (W.C. Gardiner, Jr., Ed.), p. 197, Springer, New York, 1984

11. FRANK, P. AND JUST, Th.: Ber. Bunsenges. Phys. Chem. *89*, 181 (1985)
12. BRAUN, M., HOFZUMAHAUS, A. AND STUHL, F.: Ber. Bunsenges. Phys. Chem. *86*, 597 (1982)
13. SRIDHARAN, U., KLEIN, F.S. AND KAUFMANN, F.: J. Chem. Phys. *82*, 592 (1985)
14. BAULCH, D.L., COX, R.A., HAMPSON, R.F., JR., KERR, J.A., TROE, J. AND WATSON, R.T.: J. Phys. Chem. Ref. Data *9*, 295 (1980)
15. HOMANN, K.H.: Diplomarbeit, University of Göttingen, 1961
16. EBERIUS, K.H., HOYERMANN, K. AND WAGNER, H. Gg.: Thirteenth Symposium (International) on Combustion, p. 713, The Combustion Institute, 1971
17. GOLDSMITH, J.E.M.: Twentieth Symposium (International) on Combustion, p. 1331, The Combustion Institute, 1984
18. LUCHT, R.P., SALMON, J.T., KING, G.B., SWEENEY, D.W. AND LAURENDEAU, N.M.: Opt. Lett. *8*, 365 (1983)
19. PEETERS, J. AND MAHNEN, G.: Fourteenth Symposium (International) on Combustion, p. 133, The Combustion Institute, 1973
20. BIORDI, J.C., LAZZARA, C.P. AND PAPP, J.F.: Fifteenth Symposium (International) on Combustion, p. 917, The Combustion Institute, 1974
21. LÜCK, K.C. AND THIELEN, W.: J. Quant. Spectrosc. Radiat. Transfer *20*, 71 (1978)
22. TEETS, R.E. AND BECHTEL, J.H.: Eighteenth Symposium (International) on Combustion, p. 425, The Combustion Institute, 1981
23. BECHTEL, J.H., BLINT, R.J., DASCH, C.J. AND WEINBERGER, D.A.: Comb. Flame *42*, 197 (1981)
24. CATTOLICA, R.J.: Comb. Flame *44*, 43 (1982)
25. LUCHT, R.P., SWEENEY, D.W. AND LAURENDEAU, N.M.: Comb. Sci. Techn. *42*, 259 (1985)
26. EBERIUS, K.H., HOYERMANN, K. AND WAGNER, H.Gg.: Fourteenth Symposium (International) on Combustion, p. 147, The Combustion Institute, 1973
27. VANDOOREN, J. AND VAN TIGGELEN, P.J.: Sixteenth Symposium (International) on Combustion, p. 1133, The Combustion Institute, 1976
28. JOKLIK, R.G., DAILY, J.W. AND PITZ, W.J.: Measurements of CH Radical Concentrations in an Acetylene/Oxygen Flame and Comparisons to Modeling Calculations. Paper WSS/CI 85–34 presented at the 1985 Fall Meeting of the Western State Section of the Combustion Institute, UC Davis, California, October 21–22, 1985

COMMENTS

Dr. A. Y Abdalla, Univ. of Zagazig, Egypt. Your OH, predicted at $\phi = 0.6$, is twice as much as what was measured.

Could this be due to a deficiency of the model? I expect this to occur in the rich side, not the lean side of the flame. Also, you have shown that the OH peak is sensitive to R(1):$O_2 + H + M \rightleftarrows HO_2 + M$ reactions, and not to R(2):$O_2 + H \rightleftarrows OH + O$ reactions, although R(1) and R(2) are related. Can you explain this?

Author's Reply. We are presently not able to explain this discrepancy which occurs only in the hydrocarbon systems (CH_4, C_2H_2). For the lean hydrogen flames, experiment and model agree. The main intention of the work presented was to prepare a consistent set of data suitable for modeling, in this respect the modeling results I presented should be considered as preliminary.

The sensitivity of the OH peak to $H + O_2 + M \rightleftarrows HO_2 + M$ you address was observed for the fairly low temperature hydrogen-oxygen flames diluted with Ar (T_{max} = 1350K), and not for the hydrocarbon flames with $T_{max} \sim$ 1800–2100 K.

At the low temperatures, the sensitivity to this reaction reflects the competition of the $H + O_2 \rightleftarrows OH + O$ (R2) and $H + O_2 + M \rightleftarrows HO_2 + M$ (R1) with subsequent $H + HO_2 \rightleftarrows OH + OH$ channels in the formation of OH. Due to the high activation energy of R2, a sensitivity to R1 is only likely to be noted at the low temperatures, as is indeed observed.

●

R. J. Roby, Stanford, USA. Are H and OH in partial equilibrium in your flames?

Author's Reply. Before answering your question I should like to point out that this work in the first respect aims at the measurements of reliable absolute radical concentrations, and that the modeling results I have shown should be regarded as preliminary. The question you address is also of great interest for us. Up to now, we have not evaluated partial equilibrium

relations for all the flames investigated in the experiments. As we did not measure the concentrations of all species necessary for these evaluations, they are rendered somewhat difficult.

It cannot be expected that in zones close to the burner surface partial equilibrium is established. Our calculations, based upon the Warnatz model, showed this quite clearly. Therefore, applying the partial equilibrium, hypothesis and measuring OH alone together with stable species, will *not* result in the correct H-atom concentrations in the vicinity of the burner surface.

●

K. Brezinsky, Princeton Univ., USA. I am somewhat surprised to see that the mechanism for the H_2/O_2 flame shows high sensitivity to the $H + O_2 + M \rightarrow HO_2 + M$ reaction at the conditions of low pressure and relatively high temperature that exist for the flame. Is there a reason for this sensitivity?

Author's Reply. For the 95 mbar, $\phi = 0.6$ hydrogen-oxygen flame diluted with Argon, for which I have shown the comparison of experiment and model you address, the maximum temperature was 1350 K (meaning that considerable regions of the flame were at still lower temperature). This is a temperature regime where the channels of $H + O_2 \rightleftarrows OH + O$ and $H + O_2 + M \rightleftarrows HO_2 + M$ followed by $H + HO_2 \rightleftarrows OH + OH$ are likely to compete in OH production, even at the comparatively low pressures. The sensitivity to $H + O_2 + M \rightleftarrows OH + OH$ was not noted at the higher temperatures of the hydrocarbon flames (~ 1800–2100 K), as expected.

●

A. N. Dean, Exxon Research & Energ., USA. Would you comment on the agreement of modeling CH in your C_2H_2 flame—is there much difference in the models of Warnatz and Miller, et al.?

What is the significance of the apparent mismatch in the $\phi = 1.6$ CH_4O_2 flame between calculated and observed OH?

Author's Reply. The trends in the agreement of measured and modeled CH seem to be similar for the data of Joklik et al (paper No. 105) modeled with their version of the detailed kinetic mechanism of Miller and coworkers and our data modeled with our version of the detailed kinetics employed in Warnatz's code. For lean and near stoichiometric $C_2H_2 - O_2$ low-pressure flames, the prediction of the position of the CH maxima and the shape of the CH profiles is better than in the rich flames; the absolute concentration is fairly well predicted. We did not compare the predictions of *both* models with our set of experimental data.

In this case we are not able to distinguish whether the $\leq 35\%$ mismatch between calculated and observed OH is caused by insufficient accuracy of the measured local temperatures ($\sim \pm 100$ K)—as OH is strongly temperature-sensitive—or whether the problem is on the modeling side due to maybe incomplete chemical kinetics or inadequate accuracy of kinetic parameters.